Tellus (2004), 56A, 189–201
Printed in UK. All rights reserved

TELLUS

Estimation of observation impact using the NRL atmospheric variational data assimilation adjoint system

By ROLF H. LANGLAND* and NANCY L. BAKER, *Naval Research Laboratory, Monterey, CA 93943-5502, USA*

(Manuscript received 30 July 2003; in final form 26 November 2003)

ABSTRACT

An adjoint-based procedure for assessing the impact of observations on the short-range forecast error in numerical weather prediction is described. The method is computationally inexpensive and allows observation impact to be partitioned for any set or subset of observations, by instrument type, observed variable, geographic region, vertical level or other category. The cost function is the difference between measures of 24-h and 30-h global forecast error in the Navy Operational Global Atmospheric Prediction System (NOGAPS) during June and December 2002. Observations are assimilated at 00UTC in the Naval Research Laboratory (NRL) Atmospheric Variational Data Assimilation System (NAVDAS). The largest error reductions in the Northern Hemisphere are produced by rawinsondes, satellite wind data, and aircraft observations. In the Southern Hemisphere, the largest error reductions are produced by Advanced TIROS Operational Vertical Sounder (ATOVS) temperature retrievals, satellite wind data and rawinsondes. Approximately 60% (40%) of global observation impact is attributed to observations below (above) 500 hPa. A significant correlation is found between observation impact and cloud cover at the observation location. Currently, without consideration of moisture observations and moist processes in the forecast model adjoint, the observation impact procedure accounts for about 75% of the actual reduction in 24-h forecast error.

1. Introduction

Operational weather forecast centers process and assimilate large amounts of observation data from satellite and *in situ* platforms several times each day in support of numerical weather prediction. We know, or generally assume, that observations add value to a model analysis and forecast. This is certainly true in the sense that when a large set of observations is assimilated, we believe that the analysis and forecast will be improved, at least in an average statistical sense. However, there are significant differences in the value added by various types of observations. It is thus of substantial interest to develop techniques that can be used to evaluate observation value and to understand patterns of observation impact on forecast skill.

This paper describes an adjoint-based procedure for assessing the impact of any or all observations used in a data assimilation and forecast system on a selected measure of short-range forecast error. Observation impact is calculated using adjoint sensitivity gradients and actual innovations to estimate the impact of each observation on the forecast error measure or cost function. With this procedure it is not necessary to add or remove observations from the assimilation to estimate their impact on the forecast. We do not attempt to directly assess if the observation has improved or degraded the analysis from which the forecast is started. The procedure can be used in predictability studies or applied as a diagnostic tool to monitor the assimilation and quality control of observations, and can also be used to develop more optimal observing networks. It can be used with any forecast and data assimilation system for which adjoints have been developed.

The observation impact, and hence the value of the observation in this context, depends on how the observation is used by the data assimilation system to define the initial conditions and also on rates of error growth during the forecast itself. In the assimilation procedure, the effect of an observation on the initial conditions (the ‘analysis’) depends on the accuracy of the observation, the number, type and configuration of other nearby observations, the specified observation and background error statistics, and other features of the assimilation technique. It can be assumed that every numerical weather forecast starts from initial conditions that contain some degree of error.

During the numerical forecast, any errors present in the initial conditions either propagate, decay, or grow, at rates that

*Corresponding author.
e-mail: langland@nrlmry.navy.mil

depend on the instability of the atmosphere, e.g. the potential for error growth. Observations will have the largest impact on forecast error when the observation influences the initial conditions in a dynamically sensitive location. Because localized error growth rates during the forecast can be very large (Langland et al. 2002), it is not necessary for the observation to produce a large change to the initial conditions for it to have a large forecast impact.

2. Observation sensitivity

The forecast model used in this study is the Navy Operational Global Atmospheric Prediction System (NOGAPS; Hogan et al. 1999). It is run with a spectral truncation of T79 (∼150 km horizontal resolution), and 30 vertical levels defined in sigma coordinates. The version of NOGAPS used here is an operational forecast system run at reduced resolution, but fully capable of resolving and forecasting synoptic-scale weather features when provided with accurate initial conditions. The NOGAPS adjoint includes a linearization of the dry dynamics, with simplified physics including vertical diffusion and surface sensible heat and momentum fluxes (Rosmond 1997). The adjoint model uses the same horizontal and vertical grid structure as the non-linear forecast model, but moist physical processes are not included at this time.

Observations are assimilated in a 6-h update cycle with the Naval Research Laboratory (NRL) Atmospheric Variational Data Assimilation System (NAVDAS; Daley and Barker 2001). NAVDAS performs a three-dimensional (3-D) variational data assimilation using NOGAPS background fields. All observations available in real time for operational use are assimilated in this study, including cloud- and feature-track wind observations from various geostationary satellites including *GOES* (Rao et al. 2002), Advanced TIROS Operational Vertical Sounder (ATOVS) temperature retrievals (Reale et al. 2003), rawinsondes, pibals, commercial aircraft observations, and surface data from ship, land, and buoy stations. Moisture is analyzed using a univariate technique.

The calculation of observation sensitivity is a two-step process that involves the adjoints of NOGAPS and NAVDAS. We seek the gradient $\partial J/\partial \mathbf{y}$ of a forecast error cost function J with respect to the vector of observations $\mathbf{y}$. We first define a scalar forecast error norm

$$e_f = \langle (\mathbf{x}_f - \mathbf{x}_t), \mathbf{C}(\mathbf{x}_f - \mathbf{x}_t) \rangle, \tag{1}$$

where $\mathbf{x}_f$ is a forecast and $\mathbf{x}_t$ is a verifying analysis. The model predictive variables (components of $\mathbf{x}$) are vorticity, divergence, potential temperature, and surface pressure (humidity is predicted by the model but not used in the error norm calculation). In eq. (1) $\mathbf{C}$ is a matrix of energy weighting coefficients that represents dry total energy; see, for example, Rabier et al. (1996) or Rosmond (1997).[1] The brackets $\langle , \rangle$ represent a scalar inner product $\langle \mathbf{x}, \mathbf{y} \rangle = \sum \mathbf{x}_i \mathbf{y}_i$. The error norm e_f has units of J kg^{-1}, and is summed between the lowest near-surface model level and a level near 150 hPa over the global domain. It can measure, for example, errors in position and intensity of synoptic-scale cyclones, high-pressure centers, and mid-latitude and subtropical jet streams. The forecast verification area (FVA) in which the error is calculated in this study is the global domain. To perform the adjoint sensitivity calculations, we define a cost function as

$$J_f = \frac{1}{2} e_f, \tag{2}$$

and the starting condition for the adjoint integration, valid at forecast verification time, is thus

$$\frac{\partial J_f}{\partial \mathbf{x}_f} = \mathbf{C}(\mathbf{x}_f - \mathbf{x}_t). \tag{3}$$

One integration of the forecast model adjoint provides a 3-D sensitivity vector with respect to the initial conditions of the forecast trajectory

$$\frac{\partial J_f}{\partial \mathbf{x}_a} = \mathbf{L}^{\mathbf{T}} \frac{\partial J_f}{\partial \mathbf{x}_f}, \tag{4}$$

where $\mathbf{L}^{\mathbf{T}}$ is the operator representing the adjoint of the discretized NOGAPS. The sensitivity gradient $\partial J_f/\partial \mathbf{x}_a$ can be used to estimate how J_f is changed by adding small perturbations (such as analysis errors) to $\mathbf{x}_a$. This adjoint sensitivity is obtained in a tangent linear context with respect to a trajectory provided by the non-linear global forecast model (including moist physics) that is updated every second time-step ($2\Delta t = 1800$ s). It is generally useful in short-range forecasts of 72 h or less.

The analyzed initial conditions $\mathbf{x}_a$ are produced by adding analysis increments to a background $\mathbf{x}_b$. The NAVDAS analysis (Daley and Barker 2001) is performed in observation space and can be written as

$$\mathbf{x}_a - \mathbf{x}_b = \mathbf{P}_b \mathbf{H}^T \left[\mathbf{H}\mathbf{P}_b\mathbf{H}^T + \mathbf{R} \right]^{-1} (\mathbf{y} - \mathbf{H}\mathbf{x}_b) \tag{5}$$

where $\mathbf{P}_b$ is the background error covariance matrix, $\mathbf{y}$ is the observation vector, $\mathbf{R}$ is the observation error covariance matrix, and $\mathbf{H}$ projects $\mathbf{x}_b$ into observation space. The second step in the sensitivity calculations is to extend the initial condition sensitivity gradient from the grid point form provided by eq. (4) into observation space, using the adjoint of NAVDAS

$$\frac{\partial J_f}{\partial \mathbf{y}} = \left[\mathbf{H}\mathbf{P}_b\mathbf{H}^T + \mathbf{R} \right]^{-1} \mathbf{H}\mathbf{P}_b \frac{\partial J_f}{\partial \mathbf{x}_a}, \tag{6}$$

where $\mathbf{H}\mathbf{P}_b$ is the adjoint of the post-multiplier step $\mathbf{P}_b\ \mathbf{H}^T$, and $[\mathbf{H}\mathbf{P}_b\mathbf{H}^T + \mathbf{R}]^{-1}$ is self-adjoint (following Baker and Daley 2000). The assimilation procedure is nearly linear, so the adjoint

[1]While the cost function here uses an energy weighting, the sensitivity gradient calculation does not optimize growth within an energy norm as is done with certain types of singular vectors.

calculation for NAVDAS does not involve significant tangent linear approximations.

The quantity $\partial J_f/\partial \mathbf{y}$ is the sensitivity of the forecast error cost function with respect to the complete observation vector $\mathbf{y}$, assuming that the background is held fixed (e.g. $\mathbf{x}_b$ is not perturbed). The sensitivity gradient $\partial J_f/\partial \mathbf{y}$ can be used to estimate how J_f is changed by adding small perturbations (such as observation errors) to actual or even hypothetical observations. In addition, $\partial J_f/\partial \mathbf{y}$ is the sensitivity to the innovation vector (observation–background), and in this application it provides a means for diagnosing the impact of actual observations, as described in Section 3.

It is useful to note that it is necessary to translate the sensitivity gradient $\partial J_f/\partial \mathbf{x}_a$, which is obtained on the forecast model grid in eq. (4), onto the NAVDAS analysis grid before it can be used in eq. (6). Care should be taken in this step because interpolation of sensitivity gradients must consider differences in thickness of model layers and variations in horizontal grid resolution over the model domain. Procedures that are used for interpolation of conventional fields (temperature, wind) may introduce serious distortion of sensitivity gradient fields if they do not include the appropriate weighting functions.

3. Observation impact calculation

We can adapt the sensitivity procedure described in Section 2 to address specific questions related to observation impact in the context of the actual model forecast and data assimilation cycle. For example, suppose observations are assimilated at 6-h intervals and we wish to determine the impact of observations taken at 00UTC on a scalar measure of global forecast error in a forecast of length f. Now let $g = f + 6h$, which is the length of a forecast started at the previous NAVDAS assimilation time (18UTC). The forecasts of lengths f and g both verify at the same time, t. This analysis and forecast configuration is depicted in Fig. 1.

While the forecast errors e_f and e_g are caused by inaccuracies in both the initial conditions and the forecast model, the difference between the forecast errors ($\Delta e_f^g = e_f - e_g$) is due solely to the assimilation of observations at 00UTC. If there are no observations at 00UTC, it is evident that e_f will be equal to e_g because the trajectory starting from 18UTC (−6 h) will not be changed and $\mathbf{x}_a = \mathbf{x}_b$. In the more usual case, observations will be assimilated, $\mathbf{x}_a \neq \mathbf{x}_b$, and usually $e_f < e_g$, because $\mathbf{x}_a$ is generally closer than $\mathbf{x}_b$ to the true atmospheric state.

For the purpose of evaluating observation impact it is therefore appropriate to use the forecast error difference Δe_f^g as a cost function. Using observation sensitivity gradients, Δe_f^g can be estimated as

$$\delta e_f^g = \left\langle (\mathbf{y} - \mathbf{H}\mathbf{x}_b)\,, \frac{\partial J_f^g}{\partial \mathbf{y}} \right\rangle, \tag{7}$$

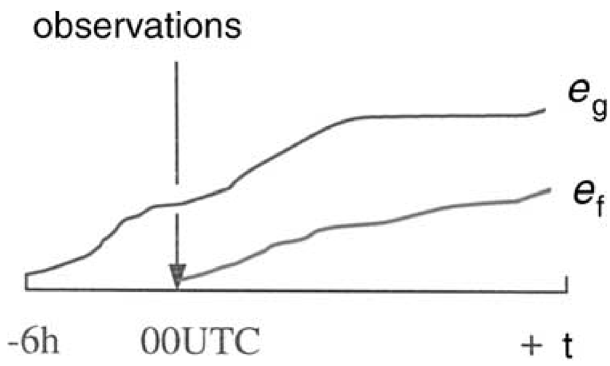

Fig 1. Observations are assimilated at 00UTC, creating initial conditions for a new trajectory, which has forecast error e_f. The old trajectory starts from 18UTC (−6 h), and has forecast error e_g. It also provides the background for the analysis at 00UTC. Both forecasts verify at time t, where t equals the length of forecast f. The difference between the errors $e_f - e_g$ is due solely to assimilation of observations.

where $\mathbf{y} - \mathbf{H}\mathbf{x}_b$ is the innovation vector. A complete derivation of the observation impact eq. (7) is provided in Appendix A, and it is noted here that to calculate δe_f^g the observation sensitivity $\partial J_f^g/\partial \mathbf{y}$ is obtained using sensitivity on two trajectories, which are the forecasts starting from 18UTC and 00UTC, respectively.[2] The quantity δe_f^g, as defined in eq. (7) provides the information we require to assess observation impact using only observation-space quantities. The accuracy of δe_f^g, and the observation sensitivity accuracy are subject to the same approximations and tangent linear limitations that apply to sensitivity obtained from the adjoint of the forecast model.

Using eq. (7) the global observation impact can be partitioned into contributions made by any individual observation or grouping of observations that may be of interest. The total global observation impact is the inner product in eq. (7) evaluated using every observation assimilated over the entire globe. Currently about 250 000 observations (excluding moisture data) are assimilated each day at the 00UTC analysis time in NAVDAS. Note that each item of temperature, wind, and pressure data is counted as a separate observation; for example, a rawinsonde profile is not ‘one’ observation but all the separate temperature, height, and wind observations at every pressure level.

4. Observation impact results

It is convenient to group the observation impact results by instrument type, such as rawinsondes, ATOVS, surface data, wind observations from geostationary satellites, or commercial aircraft observations. For example, we might wish to evaluate the combined impact of all geostationary satellite wind observations

[2]The study by Fourrie et al. (2002) also uses the error difference $e_f - e_g$ as a cost function, but their impact function uses sensitivity gradients involving one trajectory.

over the global domain. It is possible to also consider any arbitrary subset of observation data, such as only observations below 500 hPa, or only data from within a selected region. The global observation impact is the sum of all individual observation impacts for all instrument types.

4.1. Monthly results: June and December 2002

The cost function used here to estimate observation impact is the difference between quadratic measures of 24-h and 30-h forecast errors, $e_{24} - e_{30}$, over the global domain. The monthly average 24-h and 30-h forecast errors (both verifying at 00UTC) for June and December 2002 are shown in the four panels of Fig. 2. The largest forecast errors occur in mid-latitudes of the winter hemisphere in association with synoptic-scale cyclones and anticyclones. Large 24-h forecast errors are especially notable in December over the eastern North Pacific and western North America at the end of the North Pacific storm track. Note that the magnitude of this energy-weighted error field tends to decrease in high latitudes because the relative volume represented by each model grid point becomes smaller towards the poles. The global value of e_{24} is approximately 0.75 (e_{30}), on average.

Figure 3 presents the summed monthly observation impact δe_{24}^{30} for seven observation instrument types during June and December 2002, with $f = 24$ h and $g = 30$ h. The results show the extent to which the assimilation of observations at 00UTC acted to reduce (or possibly to increase) 24-h global forecast error from what the error would have been if those observations were not assimilated. In Fig. 3 the section of the shaded bar below the zero axis indicates the mean error reduction associated with the instrument type, and the section of the shaded bar above the zero axis represents the total number of those observations assimilated by NAVDAS during the month. For all observation types, the monthly summed observation impact is negative, which indicates that the observations have a beneficial impact (e.g. the forecasts starting from $\mathbf{x}_a$ have smaller errors, on average, than the forecasts starting from $\mathbf{x}_b$) when they are assimilated by NAVDAS.

During both June and December 2002 ATOVS temperature retrievals provide the largest number of 00UTC observation data for NAVDAS in a global context, but the largest reduction in 24-h global forecast error is accounted for by rawinsonde observations. The impact of rawinsondes is slightly larger during December, which is the winter month in the Northern

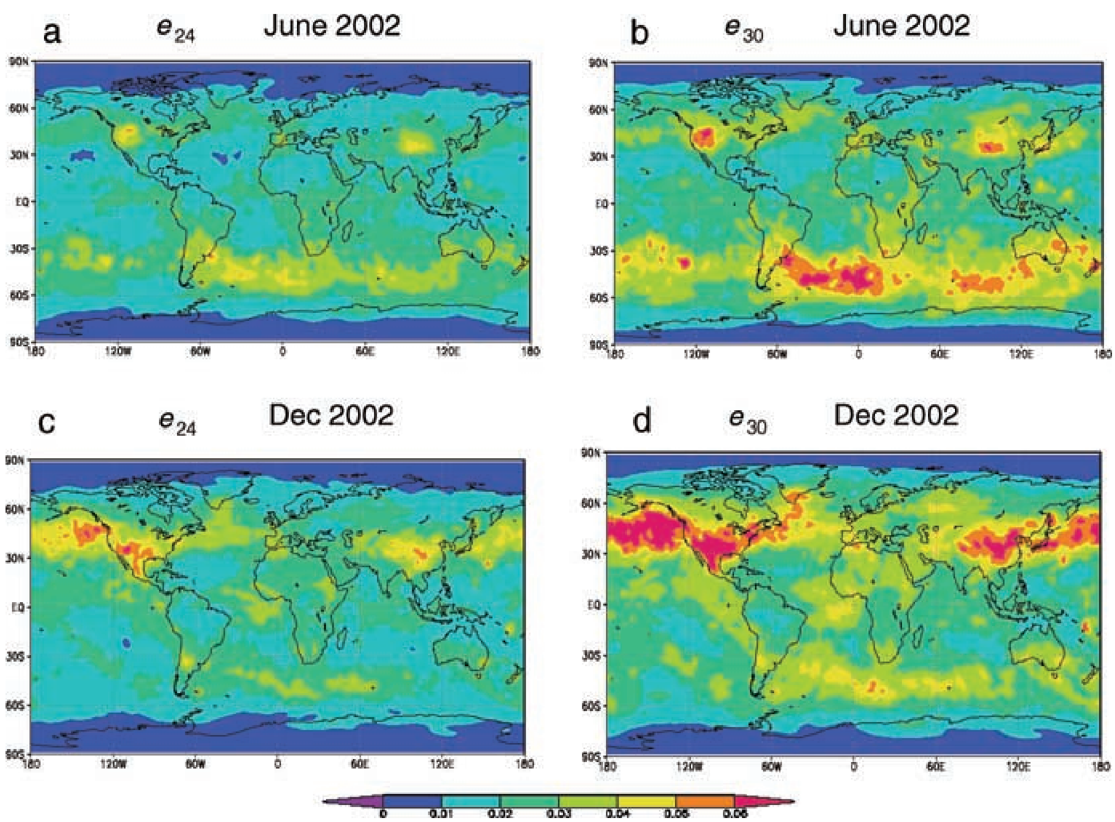

Fig 2. Average energy-weighted and vertically-integrated forecast error (J kg^{-1}) for June and December 2002. Panels (a) and (c) are 24-h forecast error, and (b) and (d) are 30-h forecast error. Errors combine temperature, wind, and pressure from near 150 hPa to the surface. Forecasts obtained with NOGAPS at T79L30 resolution and verifying analyses produced by NAVDAS.

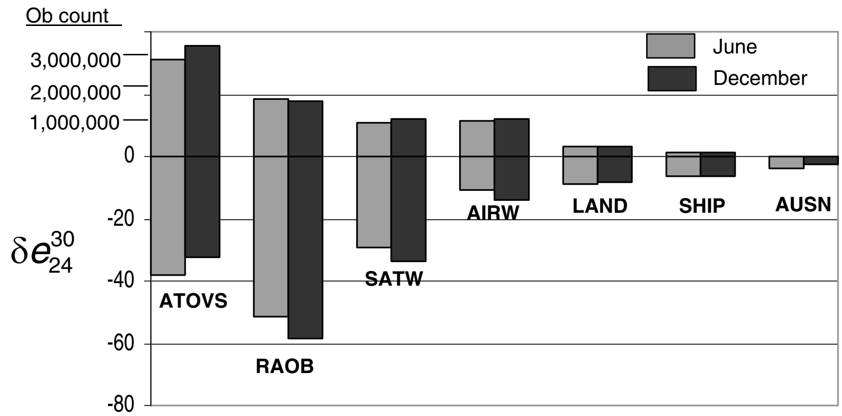

Fig 3. Summed global observation impact (δe_{24}^{30}, J kg^{-1}) for June and December 2002, partitioned by instrument type. Includes all observations assimilated in NAVDAS at 00UTC. The key is as follows: ATOVS, temperature retrievals; RAOB, rawinsondes; SATW, cloud and feature-track winds; AIRW, commercial aircraft observations; LAND, land surface observations; SHIP, ship surface observations; AUSN, synthetic sea level pressure data (Southern Hemisphere only).

Table 1. Mean observation impact (δe_{24}^{30}, J kg^{-1}), total number of observations assimilated by NAVDAS at 00UTC for the month of December 2002, and types of observation data provided

Ob type	Mean impact (per observation)	Number of observations	Variables
ATOVS	−0.9208	3 532 889	T (retrievals, super-ob, ~33 levels)
Rawinsonde	−3.3018	1 763 768	T, u, v, q (mandatory and significant levels), sea level pressure (assimilated as height)
Satellite wind	−2.7698	1 221 972	u, v (VIS, IR, WV, 500–800 hPa not assimilated)
Aircraft	−1.1612	1 203 855	T, u, v (flight level, ascent and descent)
Land surface	−2.3903	333 321	z, T, q
Ship and buoy	−6.2101	101 982	z, T, u, v, q (ship only)
Australian synthetic pressure	−31.12	7 601	Sea level pressure (assimilated as height)

Hemisphere where most rawinsondes are located. In contrast, ATOVS, which provide most of the upper-air observations in the Southern Hemisphere, have more impact in June during the Southern Hemisphere winter. Satellite wind observations and data from commercial aircraft also have substantial impact on 24-h forecast error in both June and December. Lesser impacts are associated with land and ship surface data and the synthetic sea level pressure data Guymer (1978), although the impact of AUSN per observation is relatively very large (Table 1). Ship observations, which are generally provided in data-sparse regions, also have high impact per observation, as do rawinsondes, which are heavily weighted in the assimilation procedure because of their high accuracy. In general, the impact of a particular observation on forecast error is a function of (i) location in regions where errors are large or grow rapidly, (ii) observation quality, (iii) proximity to other observations, and (iv) how well the observations are used by the assimilation procedure.

Variations in observation impact between the Northern and Southern Hemispheres (Fig. 4) are substantially greater than the seasonal variation between June and December (Fig. 3). The number and impact of *in situ* observations, primarily from rawinsonde and aircraft data, is much larger in the Northern Hemisphere. Satellite observations (primarily ATOVS and satellite wind data) are more or less evenly distributed between the hemispheres but the satellite data impact in the Southern Hemisphere is relatively large due to the sparsity of upper-air observations from rawinsondes and aircraft. Surface ship observations also have a larger impact in the Southern Hemisphere.

It is instructive to partition the results according to the vertical level of the observations, as shown in Fig. 5 for the month of December 2002. Two maxima are seen: one near the level of upper-tropospheric jet streams (200–400 hPa), and another maxima in the mid-troposphere and lower troposphere centered on the 700–800 hPa level. Approximately 40% of the total reduction in 24-h global forecast error can be attributed to observations above 500 hPa and about 60% to observations between the surface and 500 hPa, although the number of observations is larger above 500 hPa. The large number of observations in the 0–100 hPa layer are primarily ATOVS temperature retrievals in the stratosphere that do not make a substantial reduction in the measure of forecast error used for this study.

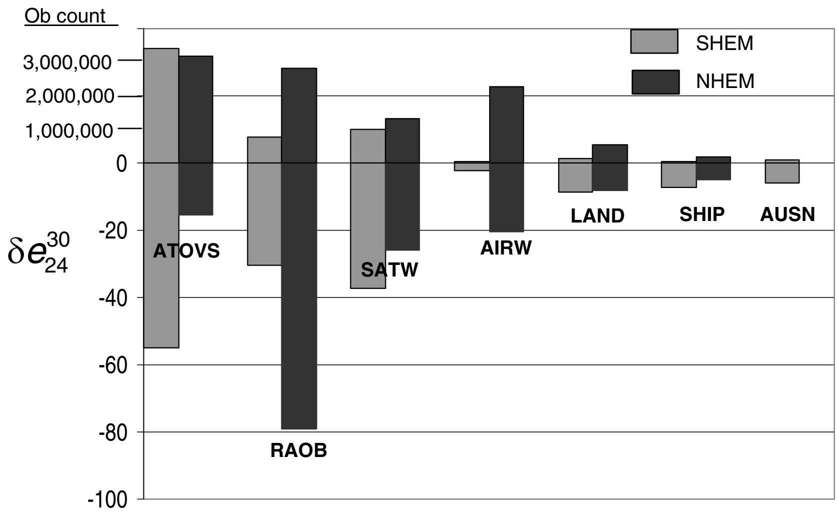

Fig 4. Summed observation impact (δe_{24}^{30}, J kg^{-1}) for Southern and Northern Hemispheres, partitioned by instrument type. Results combine June and December 2002. Includes all observations assimilated in NAVDAS at 00UTC as in Fig. 3.

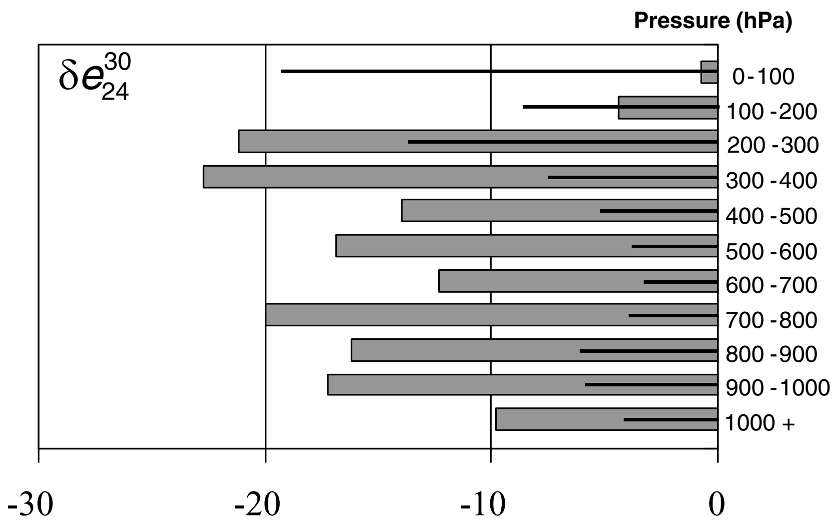

Fig 5. Summed global observation impact (δe_{24}^{30}, J kg^{-1}), partitioned by pressure level for December 2002. The black solid line within the shaded bar is proportional to the number of observations in each pressure layer. Includes all observations assimilated in NAVDAS at 00UTC as in Fig. 3.

4.2. Observation impact at 00UTC 10 December 2002

It has been shown above that the assimilation of large sets of observation data reduces short-range global forecast error. However, the impact of individual observations can vary widely, and the adjoint-based calculation allows us to quantify (or rather, to estimate with reasonable accuracy) this impact for every separate observation in the global domain at a particular analysis time. Figure 6 illustrates the observation impact δe_{24}^{30} and geographic distribution of four observation types in the NAVDAS assimilation at 00UTC 10 December 2002.

For each of the four observation types in Fig. 6, the global sum of observation impact δe_{24}^{30} at this assimilation time is negative (e.g. assimilating the observations contributes to a reduction in forecast error, $e_{24} < e_{30}$), although each instrument type contains a considerable fraction of individual observations which produce positive values of δe_{24}^{30}. This combination of negative and positive observation impact reflects the statistical nature of data assimilation, in which it is necessary to make significant assumptions and approximations about observation and background error statistics. Every observation is not used in an optimal sense, even though assimilation of complete sets of global observations usually produces a reduction in forecast error by creating a new initial condition (analysis) that is closer than the background to the true atmospheric state. Any change to the number or configuration of observations, such as adding or removing observations, will increase or decrease the impact of other observations. General assessments of observation value should be made by examining observation impact over extended time periods, because the impact and value of observations has large variability from day to day.

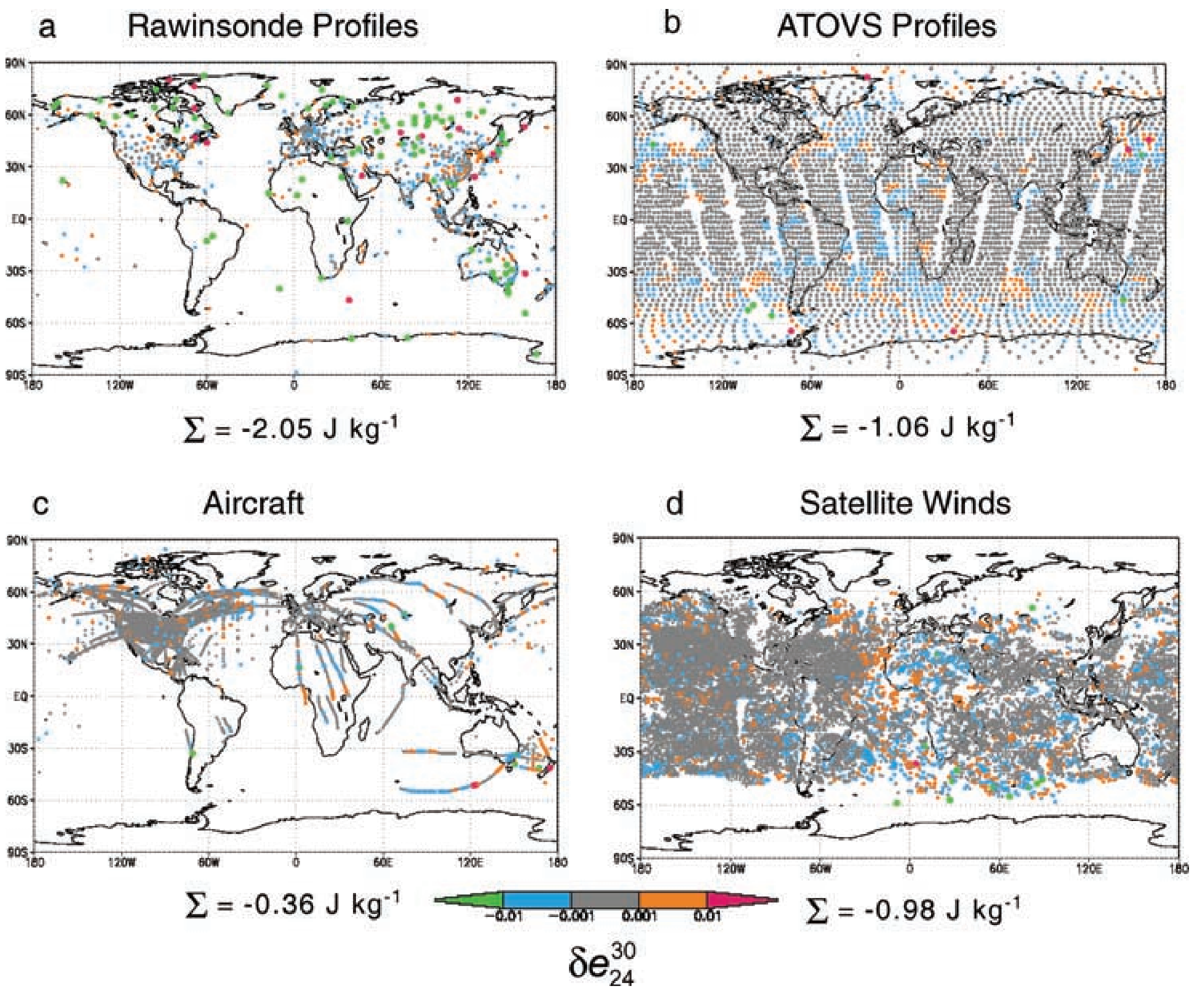

Fig 6. Observation impact (δe_{24}^{30}, J kg^{-1}) in the NAVDAS assimilation at 00UTC 10 December 2002. Green (red) dots represent large reduction (increase) in 24-h global forecast error. Blue (orange) dots represent moderate reduction (increase) in 24-h global forecast error. Gray dots represent relatively small reduction or increase in 24-h global forecast error. For rawinsondes and ATOVS, each dot represents the combined impact of observations in vertical profiles. For aircraft and satellite wind observations, each dot combines the impact of observations with the same latitude, longitude, and pressure level.

The impact of individual rawinsonde profiles can be relatively large, as indicated by the numerous green and red (large observation impact) dots in Fig. 6a. Rawinsondes along coastlines and in regions where other observations are sparse frequently have the largest observation impact, because they generally receive more weight in the assimilation procedure. The impact of individual ATOVS profiles (Fig. 6b) is generally less than that of rawinsonde profiles because the ATOVS data include only temperature and the profiles are provided in an evenly-distributed pattern that makes extremely high or low observation impacts less likely. A scatter plot (Fig. 7) illustrates the impact of this global set of ATOVS observations as a function of latitude. Although the distribution appears to be more or less evenly portioned in terms of positive and negative impacts, the global summed value of $\delta e_{24}^{30} = -1.06$ J kg^{-1} indicates that the global set of ATOVS temperature retrievals did in fact have a beneficial impact. Observations with the smallest relative impact on forecast error are represented by gray dots in Fig. 6, but it should be noted that the total impact obtained by summing large numbers of observations in the ‘small impact’ category can be substantial.

Observations provided by commercial aircraft (Fig. 6c) are quite dense over North America, where their impact is diminished to some extent because of numerous rawinsonde and land surface observations. However, the cumulative global impact of aircraft observations is still very significant and individual aircraft observations in regions of strong sensitivity can provide large observation impact. Wind data from geostationary satellites (Fig. 6d) are well distributed from about 50S to 60N and have substantial global impact, although satellite wind observations between 500–800 hPa were not assimilated in NAVDAS

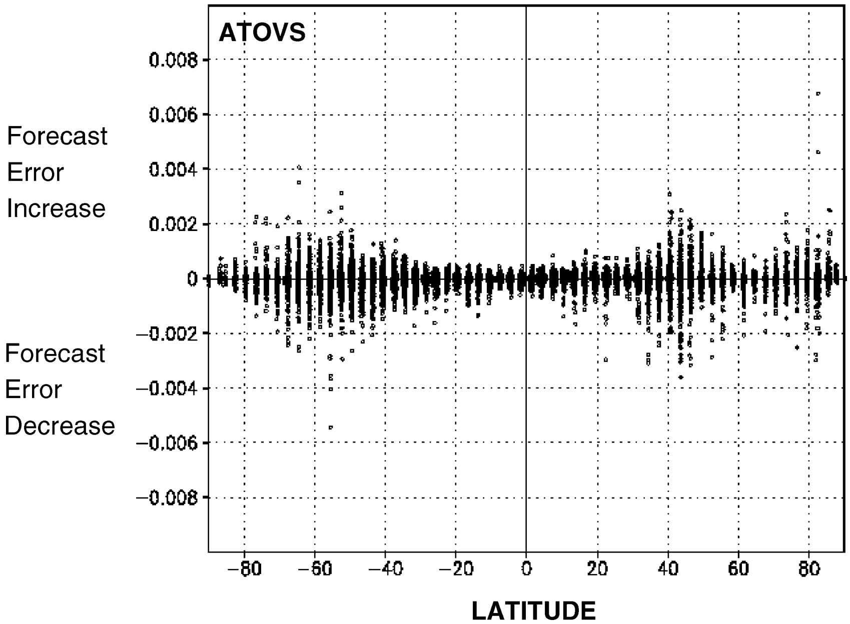

Fig 7. Observation impact (δe_{24}^{30}, J kg^{-1}) for ATOVS temperature retrievals (all vertical levels included) and latitude in the assimilation at 00UTC 10 December 2002. The number of observations in this plot is about 117 000 and the total $\delta e_{24}^{30} = -1.06$ J kg^{-1}.

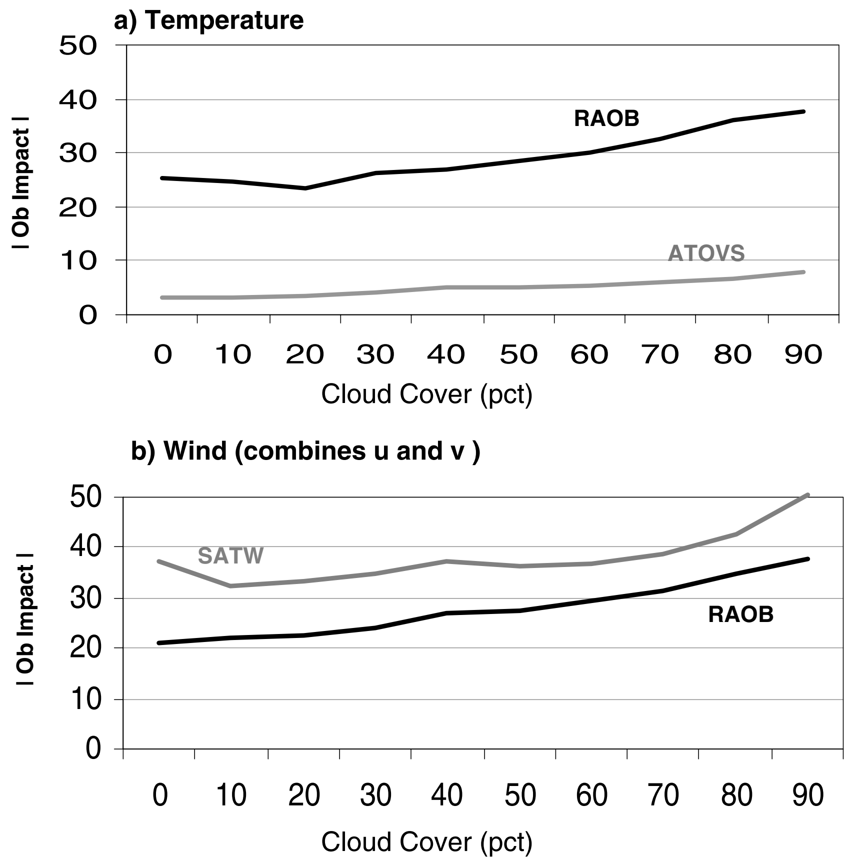

Fig 8. Mean absolute value of observation impact ($\frac{1}{N}\sum|\delta e_{24}^{30}|10^{-5}$, J kg^{-1}) and model-diagnosed total cloud cover amount. N is the number of observations. Results for the month of December 2002. Observations are: RAOB, temperature and wind from rawinsonde profiles; ATOVS, temperature retrieval profiles; SATW, cloud and feature-track wind, all in global domain.

during this period. Satellite wind data can receive large weight in the NAVDAS assimilation, and may have observation impacts as large as entire ATOVS profiles, which provide the only other upper-air observations in some oceanic areas.

4.3. *Cloud cover correlation*

There is a significant positive correlation between observation impact and cloud cover at observation locations. Figure 8 compares the mean absolute value of observation impact for temperature (panel a) and wind (panel b) as a function of model-diagnosed cloud cover. Here, cloud cover is defined as the percent of sky covered by all cloud types, including high, middle, and low clouds. It should be noted that Fig. 8 shows the magnitude of observation impact, which combines beneficial (negative) and non-beneficial (positive) observation impacts.

In Fig. 8a, it can be seen that the impact of a rawinsonde temperature observation in a location with 80% cloud cover is about 1.5 times larger than the impact in locations with 20% cloud cover. This correlation of observation impact with cloud cover likely exists because: (i) cloudy regions are more dynamically active and sensitive to analysis errors (McNally 2002), and (ii) there are fewer total observations in regions with the highest percentage cloud cover, so that each available observation there may receive more weight individually in the assimilation. The result supports the concept that targeting additional satellite or *in situ* observations into cloudy regions could be an effective means to improve forecast skill.

Figure 8a also indicates that the average magnitude of rawinsonde temperature impact is about four to five times larger than the impact of ATOVS temperature retrieval observations. This result can be explained, at least partially, by the fact that rawinsonde temperature observations have a smaller assigned observation error (1 K) in comparison to ATOVS (2.5 K at 500 hPa) and therefore rawinsonde data receive greater weight in the NAVDAS analysis. However, in a global context there are many more ATOVS than rawinsonde observations, and thus the total global impact of ATOVS data at 00UTC is roughly comparable to that of rawinsondes, as discussed in Section 4.1.

The impact of wind observations (Fig. 8b) is also correlated with cloud cover. Rawinsonde wind (Fig. 8b) and temperature (Fig. 8a) observations are approximately equal in terms of observation impact. Satellite wind observations tend to have a relatively large number of large positive and large negative impacts, so that the average magnitude of their observation impact is larger that that of rawinsonde winds. It is hypothesized that the larger impacts associated with satellite wind data are related to greater uncertainty in the observation values, which can produce larger innovations, or that isolated satellite wind data may receive greater weight in the assimilation than wind observations in rawinsonde profiles.

4.4. Accuracy of observation impact calculations

The relevance of the observation impact results depends on the accuracy of the adjoint-based error calculation defined by eq. (7). Specifically, we desire that δe_f^g provide a reasonable estimate of the 'true' value of $e_f - e_g$ obtained from the non-linear model forecasts, although it is not necessary and is not expected that δe_f^g will be exact in order for the observation impact calculations to provide useful information.

During June and December 2002, the value of $e_{24} - e_{30}$ obtained from NOGAPS forecasts (dark lines in Fig. 9) is negative each day, which indicates that the complete global set of observations assimilated at 00UTC in NAVDAS consistently produces a more accurate short-range forecast trajectory. The adjoint-based estimate δe_{24}^{30} (gray lines in Fig. 9) follows the daily trend of $e_{24} - e_{30}$ quite well, but with a magnitude that is reduced from the actual error difference by about 25% on average. This indicates that the adjoint-based estimate consistently underestimates the actual impact of observations assimilated by NAVDAS.

There are two primary reasons why the adjoint-based observation impact estimate is not more accurate. First, the calculation of sensitivity using the NOGAPS adjoint does not account for moist physics or non-linearities in the dry dynamics, which necessarily explain some fraction of short-range forecast error growth. Secondly, the calculation of observation impact using the inner product eq. (7) does not include moisture or humidity observations, which account for roughly 30% of the total global observation set.

It is not clear at this time which of the two limitations is most significant. However, given that the calculations exclude direct consideration of moisture as well as non-linear effects, it is perhaps surprising and encouraging that global observation impact can be estimated with an accuracy of even 75%. The results suggest that much of the impact that observations have on error in short-range weather forecasts can be explained by 'dry' observations (temperature, wind, and height) and quasi-linear processes in the forecast model. By inference, the assimilation of moisture observations and effects of moist physics in the forecast model appears to explain a smaller, but still significant, fraction of observation impact. It can also be noted that because we are estimating the difference between two forecast error measures provided by the same model, the issue of 'model error' (e.g. forecast errors caused by model deficiencies) is largely removed from the problem. In this context, our interest is not to determine the specific causes of forecast errors, but rather to estimate how the assimilation of observations modifies the forecast error of the background by producing an improved trajectory.

5. Summary and discussion

This paper describes a procedure for estimating the impact of observations on a measure of short-range forecast error, using adjoint versions of the forecast model and the data assimilation procedure. A significant advantage of the method is that observation impact can be efficiently estimated for a complete global set of observations or any subset of observations grouped by instrument type, observed variable, geographic region, vertical level, or other category. The computational cost

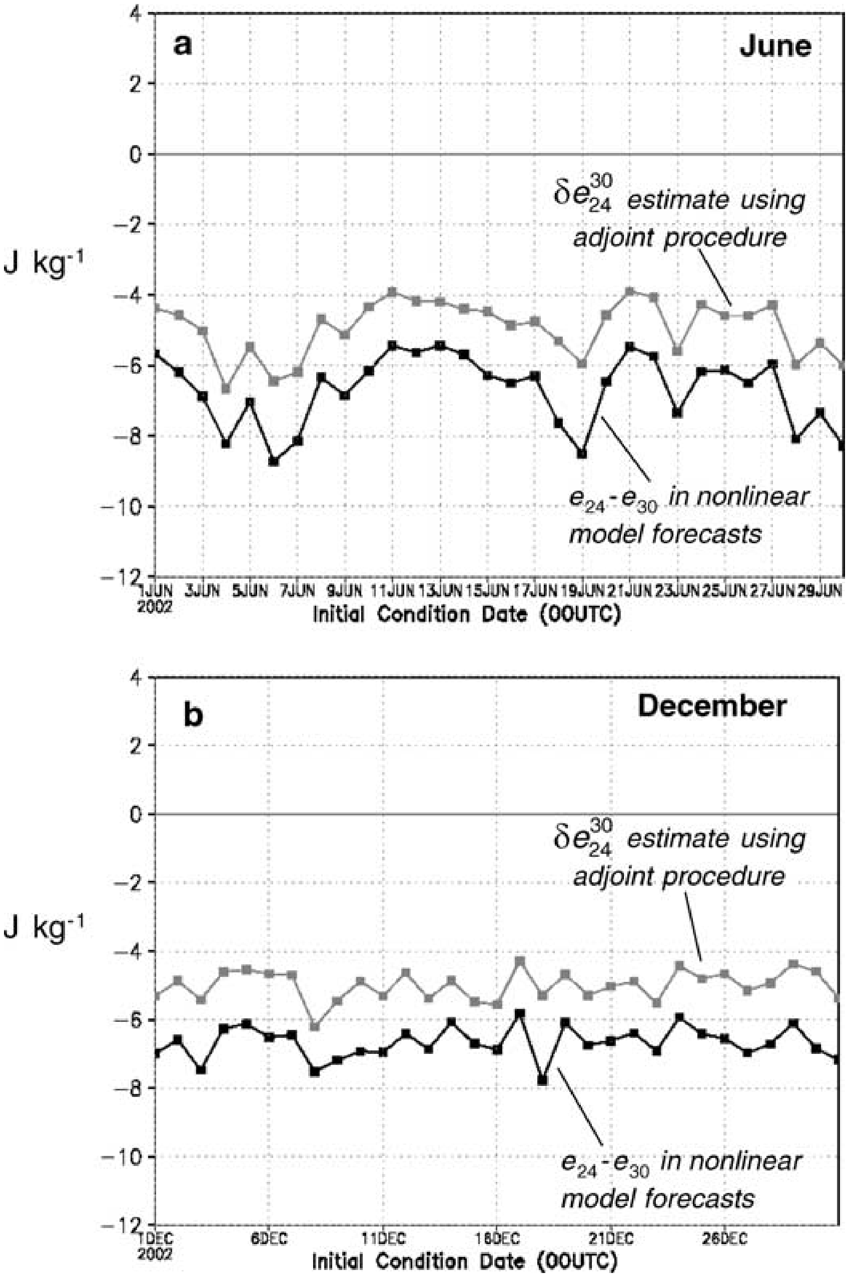

Fig 9. Time series of $e_{24} - e_{30}$ (dark solid line) in NOGAPS forecasts and corresponding adjoint-based observation impact estimate δe_{24}^{30} (gray solid line) calculated for the global domain in (a) June 2002 and (b) December 2002. Units are J kg^{-1}.

of the observation impact calculations is roughly the same as a single run of the forecast model and the data assimilation procedure.

The information about observation impact provided by this adjoint-based method can be considered complementary to that provided by conventional data-denial sensitivity experiments (Bouttier and Kelly 2001) and Observation System Simulation Experiments (OSSEs). An advantage of our method is that observation impact is evaluated without the need to selectively add or remove data, which can change the value of the remaining observations. A disadvantage is that the observation impact assessment is relevant only for the selected cost function (although many cost functions can be used), which means that the effect of observations on other aspects of the forecast is not directly described.

The cost function used in this study is the difference between quadratic measures of 24-h and 30-h forecast error, using trajectories starting from 00UTC and 18UTC, respectively. The difference in the forecast errors of these trajectories $e_{24} - e_{30}$ is due entirely to the assimilation of observations at 00UTC.

Currently, without consideration of moisture observations or moist physical processes in the adjoint calculations, we can account for approximately 75% of the actual impact of a complete global set of observations on 24-h forecast error. The method can be applied to forecasts longer than 24 h, although the accuracy will decrease because of tangent linear assumptions in the adjoint of the forecast model. Because the NAVDAS assimilation procedure is nearly linear, there is little or no loss of accuracy in the use of its adjoint.

The total impact of the global observation set is the sum of a widely-varying range of impact associated with individual observations. The combined impact of assimilating all observations over the global domain reduces $e_{24} - e_{30}$, but a substantial fraction of observations in any given assimilation increases this error measure. This is a general result that demonstrates the statistical manner in which data assimilation procedures extract value from large sets of observation data.

For observations assimilated in NAVDAS at 00UTC during June and December 2002, the largest reductions in Northern Hemisphere 24-h forecast error are provided by rawinsondes, satellite wind data, commercial aircraft data, and ATOVS temperature retrievals. In the Southern Hemisphere, the largest 24-h forecast error reductions are provided by ATOVS, satellite wind data, and rawinsondes. Lesser error reductions in both hemispheres are associated with land and ship surface data and, in the Southern Hemisphere, with synthetic sea level pressure observations.

In terms of vertical distribution, significant 24-h forecast error reductions are produced by observations in all levels of the troposphere. There is a relative maxima of observation impact in the upper troposphere (200–400 hPa), although the impact of all observations below 500 hPa is larger (60% of the total) than the impact of observations above 500 hPa (40%). There is a positive and significant correlation between the impact of individual observations and cloud cover at the observation location, which suggests that 'targeting' of supplemental observations to cloudy regions could be an effective means to reduce short-range forecast error.

The adjoint-based procedure provides an efficient and useful method for estimating observation impact. However, several cautions and caveats should be considered in the interpretation of the results.

(i) The observation impact (or 'value') of observations calculated by this method depends on the cost function (J) that is selected. We use here a quadratic measure of vertically-integrated (150 hPa to surface) and energy-weighted global forecast error that includes temperature, winds, and surface pressure. The 'impact' of observations will of course be different if other cost functions are used.

(ii) The impact of particular observations and sets of observations depends strongly on the assimilation system and forecast model. The observation impact is likely to have different magnitude, or could change sign, when other data assimilation procedures and forecast models are used, because there will inevitably be differences in observation error and background error statistics, differences in the quality of the background, and other issues.

(iii) The results shown here are based only on observations assimilated in NAVDAS at 00UTC. At other assimilation times (06UTC, 12UTC, and 18UTC) observation impact will be different because the distribution of observations is not the same as at 00UTC. For example, because the great majority of rawinsondes are provided only at 00UTC and 12UTC, the impact of satellite and other *in situ* observations will be substantially different in the assimilations at 06UTC and 18UTC.

Acknowledgments

The authors thank Tim Hogan and Thomas Rosmond for assistance in running NOGAPS and the NOGAPS adjoint systems. Ed Barker provided essential guidance with the use of NAVDAS. The first version of the NAVDAS adjoint system was developed by the late Dr Roger Daley. RL is sponsored by the NRL and the Office of Naval Research under program element 0601153N, project BE-033-03-4L. NB is sponsored under program element 0601153N, project BE-033-03-45. This paper is dedicated to Dr Roger Daley (1943–2001), visiting senior scientist at the NRL, Monterey, CA, from 1995 to 2001. We would like to thank two anonymous reviewers whose suggestions helped to improve the manuscript.

Appendix A: Derivation of expressions for δe_f^g in grid point and observation space

Consider two non-linear forecasts of lengths f and g both verifying at a time, t, for which there is a verifying analysis, $\mathbf{x}_t$. Forecast $\mathbf{x}_f$ is started from an analysis $\mathbf{x}_\mathrm{a}$, and forecast $\mathbf{x}_g$ is started 6 h earlier (corresponding to the 6-h interval of the NAVDAS data assimilation cycle). The 6-h forecast of $\mathbf{x}_g$ provides the first guess (or background, $\mathbf{x}_\mathrm{b}$) for the analysis $\mathbf{x}_\mathrm{a}$ that represents the initial conditions for $\mathbf{x}_f$. The difference between the errors of forecasts $\mathbf{x}_f$ and $\mathbf{x}_g$ is given by $\Delta e_f^g = e_f - e_g$. We wish to derive expressions (or 'impact functions') that can be used to estimate Δe_f^g using adjoint sensitivity gradients in both the grid point space of the forecast model and the observation space of the data assimilation procedure.

We first define quadratic measures of the two forecast errors using the expressions

$$e_f = \langle(\mathbf{x}_f - \mathbf{x}_t), \mathbf{C}(\mathbf{x}_f - \mathbf{x}_t)\rangle \tag{A1}$$

$$e_g = \langle(\mathbf{x}_g - \mathbf{x}_t), \mathbf{C}(\mathbf{x}_g - \mathbf{x}_t)\rangle \tag{A2}$$

where $\mathbf{C}$ is a matrix of energy weighting coefficients for dry total energy. Using eqs (A1) and (A2) we define two cost functions

$$J_f = \frac{1}{2}\langle(\mathbf{x}_f - \mathbf{x}_t), \mathbf{C}(\mathbf{x}_f - \mathbf{x}_t)\rangle \tag{A3}$$

$$J_g = \frac{1}{2}\langle(\mathbf{x}_g - \mathbf{x}_t), \mathbf{C}(\mathbf{x}_g - \mathbf{x}_t)\rangle \tag{A4}$$

and the corresponding first derivatives

$$\frac{\partial J_f}{\partial \mathbf{x}_f} = \mathbf{C}(\mathbf{x}_f - \mathbf{x}_t) \tag{A5}$$

$$\frac{\partial J_g}{\partial \mathbf{x}_g} = \mathbf{C}(\mathbf{x}_g - \mathbf{x}_t). \tag{A6}$$

The true value of $e_f - e_g$, which we will call Δe_f^g, is defined as eq. (A1) minus eq. (A2). We wish to have an expression for Δe_f^g that involves sensitivity gradients, which can be written using the gradients defined in eqs (A5) and (A6) as

$$\Delta e_f^g = \left\langle (\mathbf{x}_f - \mathbf{x}_g), \frac{\partial J_f}{\partial \mathbf{x}_f} + \frac{\partial J_g}{\partial \mathbf{x}_g} \right\rangle. \tag{A7}$$

It is easily shown that the right-hand side of eq. (A7) is equivalent to the difference in forecast errors $e_f - e_g$. Note that it is necessary to use sensitivity gradients involving both the f and g trajectories because $e_f - e_g$ is the difference between two quadratic error expressions.

The difference between the forecast trajectories f and g at initial time is $\delta\mathbf{x}_\mathrm{a} = \mathbf{x}_\mathrm{a} - \mathbf{x}_\mathrm{b}$, or the analysis minus the background. If we assume that this initial difference evolves in a tangent linear sense into a good approximation of the forecast difference $\mathbf{x}_f - \mathbf{x}_g$, then we can estimate $e_f - e_g$ using $\delta\mathbf{x}_\mathrm{a}$ and sensitivity gradients which the adjoint model has mapped back to initial time along the two forecast trajectories. Thus, the adjoint model maps $\partial J_f/\partial \mathbf{x}_f$ into $\partial J_f/\partial \mathbf{x}_\mathrm{a}$ along trajectory f and $\partial J_g/\partial \mathbf{x}_g$ is mapped into $\partial J_g/\partial \mathbf{x}_\mathrm{b}$ along trajectory g, which allows us to write

$$\delta e_f^g = \left\langle \delta\mathbf{x}_\mathrm{a}, \frac{\partial J_f}{\partial \mathbf{x}_\mathrm{a}} + \frac{\partial J_g}{\partial \mathbf{x}_\mathrm{b}} \right\rangle. \tag{A8}$$

Equation (A8) provides an estimate of $e_f - e_g$ in the grid point space of the forecast model. The result δe_f^g is not exact, although Δe_f^g in eq. (A7) is exact, because the sensitivity gradients in eq. (A8) are approximations obtained with the adjoint of NOGAPS. From eq. (A8) we can derive an equivalent expression for δe_f^g in the observation space of the analysis procedure. First, we recognize from eq. (5) that $\delta\mathbf{x}_\mathrm{a}$ is equivalent to $\mathbf{K}(\mathbf{y} - \mathbf{H}\mathbf{x}_\mathrm{b})$, where the Kalman gain matrix $\mathbf{K} = \mathbf{P}_\mathrm{b}\mathbf{H}^\mathrm{T}[\,\mathbf{H}\mathbf{P}_\mathrm{b}\mathbf{H}^\mathrm{T} + \mathbf{R}]^{-1}$ (Daley and Barker 2001). We may therefore rewrite eq. (A8) as

$$\delta e_f^g = \left\langle \mathbf{K}(\mathbf{y} - \mathbf{H}\mathbf{x}_\mathrm{b}), \frac{\partial J_f}{\partial \mathbf{x}_\mathrm{a}} + \frac{\partial J_g}{\partial \mathbf{x}_\mathrm{b}} \right\rangle. \tag{A9}$$

Now, because $\mathbf{K}$ is essentially linear, we can use the general definition of an adjoint operator $\langle \mathbf{K}\mathbf{y}, \mathbf{x}\rangle = \langle\, \mathbf{y}, \mathbf{K}^\mathrm{T}\mathbf{x}\rangle$ to write

$$\delta e_f^g = \left\langle (\mathbf{y} - \mathbf{H}\mathbf{x}_\mathrm{b}), \mathbf{K}^\mathrm{T}\left(\frac{\partial J_f}{\partial \mathbf{x}_\mathrm{a}} + \frac{\partial J_g}{\partial \mathbf{x}_\mathrm{b}}\right) \right\rangle. \tag{A10}$$

The operator $\mathbf{K}^\mathrm{T}$ represents the adjoint of the data assimilation procedure, which defines a sensitivity gradient in observation space

$$\frac{\partial J_f^g}{\partial \mathbf{y}} = \mathbf{K}^\mathrm{T}\left(\frac{\partial J_f}{\partial \mathbf{x}_\mathrm{a}} + \frac{\partial J_g}{\partial \mathbf{x}_\mathrm{b}}\right). \tag{A11}$$

Using eq. (A11) to substitute into eq. (A10) we obtain eq. (7) used in Section 3

$$\delta e_f^g = \left\langle (\mathbf{y} - \mathbf{H}\mathbf{x}_\mathrm{b}), \frac{\partial J_f^g}{\partial \mathbf{y}} \right\rangle, \tag{A12}$$

which involves only observation space quantities. The accuracy of the observation impact calculated in observation space eq. (A12) is essentially equivalent to the grid point space calculation eq. (A8). Unless noted otherwise, δe_f^g in this paper is evaluated using eq. (A12).

References

Baker, N. L. and Daley, R. 2000. Observation and background adjoint sensitivity in the adaptive observation targeting problem. *Q. J. R. Meteorol. Soc.* **126**, 1431–1454.

Bouttier, F. and Kelly, G. 2001. Observing system experiments in the ECMWF 4D-Var data assimilation system. *Q. J. R. Meteorol. Soc.* **127**, 1469–1488.

Daley, R. and Barker, E. 2001. *NAVDAS Source Book 2001*. NRL/PU/7530-01-441. Available from the Naval Research Laboratory, Monterey, CA, 163 pp.

Fourrie, N., Doerenbecher, A., Bergot, T. and Joly, A. 2002. Adjoint sensitivity of the forecast to TOVS observations. *Q. J. R. Meteorol. Soc.* **128**, 2759–2777.

Guymer, L. 1978. Operational application of satellite imagery to synoptic analysis in the Southern Hemisphere. Technical Report No. 26, Bureau of Meteorology, Melbourne, Australia.

Hogan, T. F., Rosmond, T. E. and Pauley, R. L. 1999. The navy operational global atmospheric prediction system: recent changes and testing of gravity wave and cumulus parameterizations. In: *Proceedings of the 13th Conference on Numerical Weather Prediction*, Denver, CO, Am. Meteorol. Soc., 60–65.

Langland, R. H., Shapiro, M. A. and Gelaro, R. 2002. Initial condition sensitivity and error growth in forecasts of the 25 January 2000 East Coast snowstorm. *Mon. Wea. Rev.* **130**, 957–974.

McNally, A. P. 2002. A note on the occurrence of cloud in meteorologically sensitive areas and the implications for advanced infrared sounders. *Q. J. R. Meteorol. Soc.* **128**, 2551–2556.

Rabier, F., Klinker, E., Courtier, P. and Hollingsworth, A. 1996. Sensitivity of forecast errors to initial conditions. *Q. J. R. Meteorol. Soc.* **122**, 121–150.

Rao, P. A., Velden, C. S. and Braun, S. A. 2002. The vertical error characteristics of GOES-derived winds: description and experiments with numerical weather prediction. *J. Appl. Meteorol.* **41**, 253–271.

Reale, A. L., Chalfant, M. L., Allegrino, A. S., Tiley, F. H., Gerguson, M. P. et al. 2003. Advanced-TOVS (ATOVS) sounding products from NOAA polar orbiting environmental satellites. In: *Proceedings of the 12th Conference on Satellite Meteorology and Oceanography*, Long Beach, CA, paper JP1.15.

Rosmond, T. E. 1997. *A Technical Description of the NRL Adjoint Modeling System*. NRL/MR/7532/97/7230. Available from the Naval Research Laboratory, Monterey, CA, 62 pp.